

Electron-enhanced desorption influence on to SPT isolator wall erosion processes

IEPC-2007-8

*Presented at the 30th International Electric Propulsion Conference, Florence, Italy
September 17-20, 2007*

Sergey S. Elovikov*
Moscow State University (MGU) Moscow, Russia

and

Sergey A. Khartov§
Moscow Aviation Institute (State University of Aerospace Technologies) MAI, Moscow, Russia

Abstract: One of the factors influences on to formation process of relief periodical structure of the output edge of SPT isolator during long time operation is a process of electron impact with the walls. It is set up a hypothesis about leading role of electron-enhanced desorption (EED) in the process of ceramics sputtering in SPT. In this paper it is represented the results of experimental investigation of electron-enhanced desorption of poly-crystal boron nitride and ceramic materials obtained on its base (BN cubical and wurtzite modifications, BN+Si₃N₄ and BN+SiO₂). Summarizing the experimental campaign authors can make the conclusion that under the typical values of electron energies in the SPT channel the electron-enhanced desorption have not play a vital part in the ceramic sputtering and therefore can be leave out during experimental and numerical modeling of SPT ceramic erosion.

Nomenclature

σ	= process cross section
σ_{TEED}	= thermal electron-enhanced desorption cross section
σ_{EED}	= electron-enhanced desorption cross section
ϕ_i	= ionicity
q	= flux of desorbing particles
e	= electron charge
j	= electron current density
N_S	= surface density of anions
I_{EDD}	= electron-enhanced desorption probability (a number of desorbing particles per one incident electron)
T	= surface temperature
D	= electron irradiation dose

I. Introduction

One of the factors influences on to formation process of relief periodical structure of the output edge of SPT isolator during long time operation is a process of electron impact with the walls. It is set up a hypothesis about leading role of electron-enhanced desorption (EED) in the process of ceramics sputtering in SPT¹.

As is known, the electrons of subthreshold energies interacting with the surfaces of some multicomponent materials cause the electron-enhanced desorption². Under the term EED we understand a process of the material destruction with certain components' desorption under the action of electrons. Desorption often modifies the

* Leading Scientists, Physical Electronics Department, College of Physics, elovikov@phys.msu.ru

§ Leading Scientist, Electric Propulsion and Space Power Plants Department, k208@mai.ru

subsurface layers and EED depends on the material nature and experimental conditions, but mainly on the sample temperature³.

The most reliable method of EED detection is undoubtedly the mass-spectral recording of desorbed particles. The fluxes about 10^{10}cm^{-2} can be measured at the mentioned limits of detection ($5\cdot 10^{-9}$ Pa), which corresponds to the EED cross-section $\sigma\sim 10^{-22}\text{cm}^2$ at electron current density ($j\sim 10^4\mu\text{A}/\text{cm}^2$). But there is an experimental problem. Since the desorbed particles of analyzed materials are the same as those of the chamber residual gas components, it is difficult to separate them. Thus, a molecular nitrogen flux is about 10^{12}cm^{-2} even at the pressure about $4\cdot 10^{-7}$ Pa should maintain during experiments.

In our work we used Auger electron spectroscopy as the simplest method of the EED cross section determination. This method is considered in work³ in details as applicable only within the limited temperature range, where the surface composition does not recover due to particle diffusion from the bulk and sorption from the gas.

The energy of radiating ions (1-3 keV) were chosen from one point of view - considering the fact that in this case it is possible to record Auger lines from all components and admixtures, forming object's composition; from other point of view - to create conditions under which there is no surface charging that corresponding to the values of secondary electron emission (SEE) $\delta>1$ (during measurements it was determined that such mode was possible under $E=1-3$ keV). It is known only one mechanism applicable to such objects - Auger neutralizing mechanism, the initial stage of which is a process of ionization of cation upper level (in our case B and Si) which is effective under electron energies higher than hundred eV. Due to mentioned causes it is not reasonable to use electrons with energies less than 1 keV.

In this work BN cubical and wurtzite modifications, $\text{BN}+\text{Si}_3\text{N}_4$ and $\text{BN}+\text{SiO}_2$ ceramics resistance – ability against low-energy radiation were investigated.

II. Electron-Enhanced Processes at the Surface of Polycrystalline Boron Nitride

As is known, electrons of subthreshold energies interacting with surfaces of some multicomponent materials cause the electron-enhanced desorption (EED)². Under the term EED we understood the material destruction with certain components' desorption under the action of electrons. This desorption often significantly modifies subsurface layers, depending on the material nature and experimental conditions, mainly on the sample temperature³.

The EED proceeds most efficiently in alkali halide compounds, where its cross section for anions reaches $\sigma = 10^{-17} - 10^{-16}\text{cm}^2$. In these cases the EED is sufficiently well explained by the model of the anion desorption due to the decay of radiationless excitons produced by electrons².

The EED is less efficient in oxides with the highest oxidation of cations ($\sigma = 10^{-21} - 10^{-20}\text{cm}^2$)^{3,7}. According to the work⁸, the basic criterion for EED on such oxide surfaces is the condition $\phi > 0.5$.

Then the anion neutralization (hence, desorption also) is possible due to the Auger processes, while the reneutralization is low-probable, since cations surrounding the anion are devoid of valence electrons. This Knotek-Feibelman model (KF model) suggests the desorption not only of neutral ions, but also positive ones, which is entirely confirmed experimentally.

If one considers the Auger neutralization leading most probably to anion emission, a simple calculation could show that the KF model for oxygen desorption well agrees to experiments quantitatively. The EED cross-section is defined by:

$$\sigma = \frac{q \cdot e}{j \cdot N_S}, \quad (1)$$

Then the EED probability, or a number of desorbing particles per one incident electron is ($N_S \sim 10^{15}\text{cm}^{-2}$ at low irradiation doses, i.e., N_S corresponds to the anion concentration at the undamaged surface):

$$I_{EED} = \frac{q \cdot e}{j} = \sigma N_S \quad (2)$$

For $\sigma = 10^{-21} - 10^{-20}\text{cm}^2$, we have $I_{EED} = 10^{-6} - 10^{-5}$, i.e., it coincides to the Auger process probability.

For covalent-bond materials the EED is also probable, however such phenomena were extremely rarely observed experimentally⁹. Meanwhile, it is assumed that the withdrawal of collectivized electrons (binding the covalent compounds), as in the KF model, is most probably related to the primary excitation of shell levels rather than to the direct excitation of valence electrons¹⁰.

The aim of this part of the work is undertake an attempt to detect experimentally the EED from the boron nitride surface using the conventional Auger spectroscopy and mass spectrometry techniques.

III. Experimental Set Up and Procedure

Since the processes leading to the EED occur in the thinnest subsurface layers, vacuum conditions and preliminary cleaning are of most importance. The fig. 1 sketches an experimental ultrahigh-vacuum facility. Experimental chamber 1 was evacuated by oil-free pumps up to pressure $P \sim 10^{-8}$ Pa. An operating vacuum was slightly poorer ($P \sim 4 \cdot 10^{-7}$ Pa) due to gas desorption on electron bombardment of the various setup units and their heating during operation. The oil-free pumping diminishes hydrocarbon content, which in turn reduces the growth rate of carbon-contained films on the bombarded surfaces. Sample 2 was placed at holder 3 mounted at manipulator moving along the three mutually perpendicular directions and rotating into the positions a, b, and c. That furnished alignment, ion cleaning (position a), and measurements by mass spectrometer 5 (position b) and Auger spectrometer 6 (position c). Apart from ion etching, samples were cleaned also by long-term high-temperature (about 1500 K) annealing with the use of a special electron-heating device. Electron guns 7 and 8 were used to irradiate samples by electron beams with energies of 400-3000 eV and current densities of $3 \cdot 10^2 - 3 \cdot 10^4 \mu\text{A}/\text{cm}^2$. An "MKh-7304" mono polar mass spectrometer with the nitrogen detection limits about $5 \cdot 10^{-9}$ Pa was used to record the EED particle fluxes. To study desorbing particles, the mass spectrometer was reconstructed: the monopolar analyzer was extremely approached to the sample, and the ionization chamber was rebuilt to furnish free particle passage through the analyzing field.

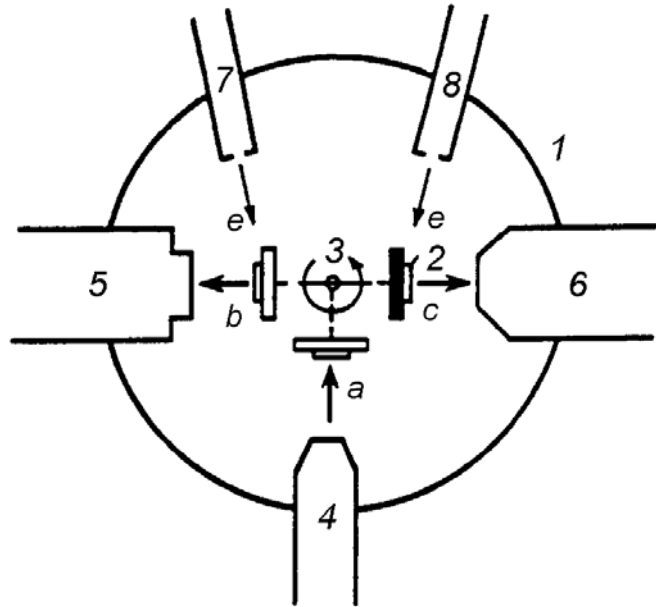


Figure 1. Diagram of the experimental facility.

ultrahigh-vacuum chamber (1), sample (2), sample holder (3), ion gun (4), mass spectrometer (5), energy analyzer of the Auger spectrometer (6), and electron guns (7, 8); various operation positions of the target (a, b, c).

The surface composition was controlled by an Auger spectrometer with the cylindrical mirror analyzer of a resolution about 0.5%. The spatial resolution specified by the electron probe diameter was about 0.3 mm.

The most reliable method of EED detection is undoubtedly the mass-spectral recording of desorbed particles. The fluxes about 10^{10}cm^{-2} can be measured at the mentioned limit of detection ($5 \cdot 10^{-9}$ Pa), which corresponds to the EED cross-section $\sigma \sim 10^{-22} \text{cm}^2$ at our electron current density ($j \sim 10^4 \mu\text{A}/\text{cm}^2$).

Since the desorbed particles are the same as those of the chamber residual gas components, ordinary difficulties arise to detect a low signal against the high background. Thus, a molecular nitrogen flux is about 10^{12}cm^{-2} even at the pressure about $4 \cdot 10^{-7}$ Pa maintained during experiments. The mass-spectral analysis shows that the signal relevant to the atomic flux (including also twice ionized nitrogen molecules) is lower than the molecular one by an order of magnitude and higher by the same value than the limit of detection. Actually, the desorption with the cross section higher than 10^{-21}cm^2 can be detected. Great difficulties emerge when determining the absolute fluxes, hence the EED cross-sections.

In the work⁶, a σ_{TEED} determination method is proposed by analyzing the thermodesorption spectra measured after a preliminary sample irradiation by electrons. As a result of the EED of one component, the surface is enriched by another, which evaporates at subsequent heating. The EED cross-sections are calculated then via the dose dependencies of the thermodesorption peaks' areas.

This simple method of the EED cross section determination is based on studying the dependence of surface concentration of desorbed particles on the electron irradiation dose. This concentration can be determined from the Auger spectra. This method is considered in the work³ in details as applicable only within the limited temperature range, where the surface composition does not recover due to particle diffusion from the bulk and sorption from the gas.

One more technique to estimate σ_{EED} is proposed in the work⁷. It was used to study the EED from the ion-bond compounds LiF and ZrO_2 . In this case the surface is enriched with the metal during anion desorption and the metal phase can be formed at a certain dose, which is evidenced by new lines appearing both in the electron energy loss and Auger spectra.

The electron-enhanced desorption of the real ceramics materials were carried out with modified «Varian» facility supplied with Auger – spectrometric device with “cylindrical mirror” type analyser with resolution over energies $\sim 0,5\%$. In the test facility it was super vacuum with residual gases pressure not higher than $P = 10^{-9}$ mbar. Electron Auger spectrums were obtained in the differentiated form in the range of electron energies $E=1000 - 3000$ eV, that is secured Auger – lines recording for all main components and admixtures. Flow density of the electron beam was $\sim 8 \cdot 10^{15}$ 1/cm²·s. Test facility block-scheme is represented in fig.2:

The sub – layer with the sample (1) was placed at the precision manipulator, securing a displacement over horizontal axis on ± 10 mm and over vertical axis on ± 20 mm with the accuracy 0.1 mm and also rotation over vertical axis. The sample cleaning was carried out under ion bombardment. As a ion source it was used the gun "Varian" (2) with electron impact ionization ($E=3$ keV, $j=0-20$ $\mu\text{A}/\text{cm}^2$). For its operation the chamber was filled by Xe with pressure up to $5 \cdot 10^{-5}$ mbar. The sample was bombarded from the electron gun (3). Ion current was measured with the help of Faraday cylinder (4). The sample was heated by tungsten-rhenium spiral (5). The temperature was measured by K-type thermo-couple (6) in the range of 20°C up to 1600°C .

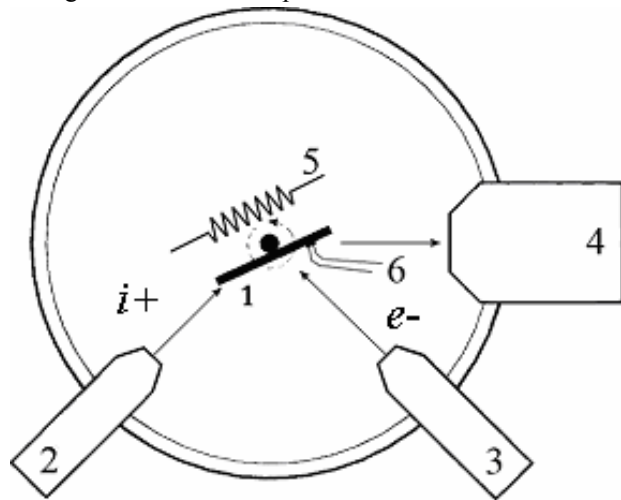


Figure 2. Modified test facility block-diagram
1- sub-layer with the sample, 2- ion source, 3 – electron gun, 4 - Faraday cylinder, 5 – heater, 6 – thermo-couple.

The sample was prepared by the following way. The samples were fixed at the manipulator and were put into vacuum chamber. When pressure level equal to $P \sim 10^{-9}$ mbar was obtained, the samples were subjected to thermo-processing (high-temperature annealing is about 1500 K, by 100° below than the boron nitride destruction onset) and ionic etching. After several cycles of heating and cleaning, the surface composition was investigated with the help of Auger spectroscopy. In this case we found out that the surface was insignificantly contaminated by oxygen. Then the samples were heated up to fixed temperatures, under which the Auger lines of the main components and admixtures were recorded (until the main impurity (carbon) content reduced to about 2%).

The energy of radiating ions (1-3 keV) were chosen from one point of view - considering the fact that in this case it is possible to record Auger lines from all components and admixtures, forming object's composition; from other point of view - to create conditions under which there is no surface charging that correspond to the values of secondary electron emission (SEE) $\delta > 1$ (during measurements it was determined that such mode is possible under $E=1-3$ keV). It is known only one mechanism applicable to such objects - Auger neutralizing mechanism, the initial stage of which is a process of ionization of cation upper level (in our case B and Si) which is effective under electron energies higher than hundred eV. Due to mentioned causes it is not reasonable to use electrons with energies less than 1 keV. It is impossible to use direct methods of investigations of EED causing objects desorption, as far as the cross section of EED is too small.

Choosing the energy of the irradiating electrons, it was considering the following:

1. It is possible to record Auger lines from all components and admixtures belonging to sample composition.
2. To create the conditions under which the surface does not charge. It is taken place under the values of secondary electron emission $\delta > 1$. During the measurements it was found out that such mode is possible under electron energy greater than 1keV.
3. To choose optimal energy of irradiating electrons.

Lets point out that the only one mechanism of electron-stimulated desorption applying to the objects similar to the investigated ceramics is Auger – neutralizing mechanism. The initial stage of this mechanism – ionization of cation top level (in our case B and Si), which is effective under electron energies higher than dozens of eV. So, it is not reasonable to use electrons with less energy, if one investigates ceramic EED. It was chosen the energy of irradiating electrons $E = 3$ keV.

Let's point out, that it was not possible to use direct methods of investigation of electron-stimulated desorption causing object destruction as far as the EED cross section of the investigated ceramics is small. Due to this fact, as it was mentioned before, a procedure based on surface properties changes recording with the help of electron Auger spectroscopy was used.

Besides, it is investigated EED of the sample consisting of the mixture: cubical (50%) and wurtzite (50%) modifications of BN. It was shown that low-energy electron action stimulates the desorption process of nitrogen atoms from the surface. The estimations concerning process cross section σ showed that under $T = 1200$ K $\sigma =$

$1,5 \cdot 10^{-22} \text{ cm}^2$, that is less approximately in one order than it is for typical EED cross sections with the surface of most oxides. Under less temperature we did not see a new Auger line. At the same time the carbon content increased greatly on the surface during electron radiation. Under high temperatures ($>1600 \text{ K}$) there was a thermo – destruction of BN with nitrogen emission and surface metallization.

Electron – stimulated desorption of BN-containing ceramics (BN+Si₃N₄ and BN+SiO₂, which are interesting as a materials for the ERT) were investigated. The examination was carried out under the temperatures close to the operational ones ($T \sim 900\text{K}$). All measurement were carried out at the fresh chips of ceramics containing a mixture of BN of hexagonal modification and SiO₂ (10% content) and Si₃N₄ (50% content) in super-vacuum ($P \sim 10^{-10} \text{ mbar}$) at «Varian» test facility with Auger-spectrometric additional device and with an analyser of “cylindrical-mirror” type.

IV. Experimental Data Analyze and Discussion

A. Investigation of Pure BN

Earlier we studied the stability of hexagonal (*h*-BN) and rhombohedral (*r*-BN) boron nitride to electron and ion irradiation^{11,12}.

It was shown that a long-term ion bombardment modifies the surface, which was evidenced by Auger spectra variations. However, we could not conclude unambiguously about on the EED of components. All the BN modifications (wurtzite (*h*-BN) and cubic (*c*-BN) together with the above mentioned) are usually recognized as preferably covalent compounds. This is evidenced, e.g., by the low ionicity $\phi_i = 0.22-0.34$, determined by various techniques for *h*-BN and *c*-BN^{13,14}. At the same time, according to other data, the ionicity of wurtzite BN is slightly exceeds 50%¹³. In this case the EED can proceed due to the Auger neutralization of anions.

The limitation to EED within the KF model, according to which the EED is possible only at $\phi_i > 50\%$, is pure conventional. It means a significant probability decrease for the KF-mechanism desorption during the ion-to-covalence binding transition.

It is very difficult to produce pure *h*-BN and *c*-BN, therefore we studied available poly crystalline objects representing a mixture of wurtzite and cubic boron nitride.

The electron irradiation was carried out at the two sample temperatures $T_1 = 300 \text{ K}$ and $T_2 = 1200 \text{ K}$ in all cases. The high temperature eliminated an additional carbon contamination of samples at the highest irradiation doses.

Now we briefly enlarge on the data acquired by using every method. Using the first technique, we could not detect nitrogen atoms desorbed from the surface. Therefore, the EED is either absent at all or the cross section is lower than 10^{-21} cm^2 , according to the above estimates.

The second mass-spectral technique appeared to be inapplicable to our case, since boron nitride began to dissociate at substantially lower temperatures before evaporation.

The attempts to detect the EED of nitrogen by using the technique measuring the surface concentration of desorbed atoms was also unsuccessful, since the Auger peaks of nitrogen were found to be independent of the irradiation dose (see fig. 3 and 4). That could evidence for the EED absence, however, as was already mentioned, the unchanged surface composition could be also explained by its restoration due to nitrogen diffusion from the bulk to the surface and adsorption from the gas phase.

A single method, allowing good reproducibility and unambiguous conclusions, was the technique for recording the metal phase formed at the boron nitride surface after electron irradiation. The Auger spectroscopy enables one to make it easily only in the case, when the main Auger lines (KVV) of BN compound and metal boron are different in energy by a value larger that the energy analyzer resolution. In our case the latter is about 1 eV at the energy corresponding to the Auger line of boron (about 180 eV).

Analysis of the energy schemes of boron and boron nitride deduced from X-ray^{15,16} and X-ray photoelectron spectra¹⁷ showed that the KVV line of metal boron should be shifted by 10 eV toward high energies. It should be also noted that X-ray K- emission spectra for *h*-BN were first measured by Fomichev¹⁶, but they are used up to now due to high reliability and informativity (self-descriptiveness).

Fig. 3 plots the Auger spectra of metal boron and boron nitride film from¹⁸. They are interpreted using the f -emission spectra of boron in boron nitride from the cited paper¹⁶.

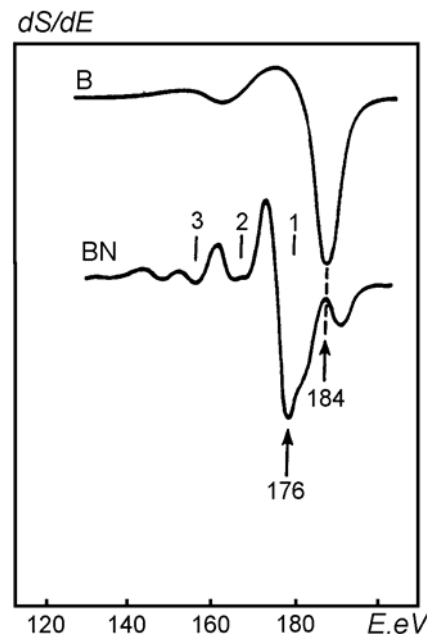


Figure 3. Auger boron lines for metal boron and boron nitride film¹⁸.

According to work¹⁸, turning points 1, 2, and 3 correspond to Auger processes KVV, KL₁V, and KL₁L₁(L₁ is the 2s level of nitrogen). It is also seen from fig. 3 that the KVV line for metal boron is shifted by about 8eV as compared to that for boron nitride, which complies with the above estimates.

Fig. 4 shows the Auger spectra measured for a sample studied at about 1200 K. The spectra are recorded immediately after surface cleaning (a) and after irradiation by electrons with the doses $8 \cdot 10^{19}$ (b) and $5 \cdot 10^{20} \text{ cm}^{-2}$ (c).

In spectrum (d) a step at the KVV boron line is observed, as spaced by 8eV from the main maximum. When the dose was increased up to $5 \cdot 10^{20} \text{ cm}^{-2}$ (Fig. 3, spectrum c), an isolated peak is already pronounced at the same energy.

Fig. 5 presents the Auger spectra for the same sample, as in fig. 4, but at room temperature, as measured before (a) and after electron irradiation with the dose $5 \cdot 10^{20} \text{ cm}^{-2}$ (b). In this case the KVV line does not change its shape, but the carbon line intensity grows. Simple estimates show that the carbon concentration rises from 2 to 6% during the irradiation.

We reason that the BN surface modification under the electron impact at high temperature ($T = 1200 \text{ K}$) is related to the electron-enhanced nitrogen desorption. This enriches the surface with boron, to form the metal phase, which is detected by the Auger spectroscopy as the new line of energy 179 eV, typical for metal boron. This can be confirmed by the following:

(i) The shift of the Auger line (179 eV) appearing on irradiation relative to the boron line (171 eV) in the nonirradiated sample is about 8 eV, which precisely corresponds to shifting the Auger peaks for metal boron and boron nitride (fig. 3).

(ii) The Auger spectra measured by us in the nonirradiated BN sample at $T > 1600 \text{ K}$ also exhibit the second line of energy 179eV. Taking into account that the compound dissociates, emitting nitrogen at such temperatures, the new line is easily explained by the metal boron phase formation.

The absence of such splitting in the spectrum of a cold sample is most probably related to retarding or suppressing the EED due to the carbon film growing on electron bombardment, which is well seen from fig. 5

The EED cross-section for nitrogen was calculated as $1.5 \cdot 10^{-22} \text{ cm}^2$ by the formula of work⁷. It is not surprising that the EED of nitrogen was not detected by mass spectrometry, since the relevant limit of EED detection is $\sigma \sim 10^{-21} \text{ cm}^2$.

When applying the KF model to the EED of nitrogen from the BN surface, the small cross section as compared to oxides can be explained by two causes. One is related to the lower ionicity of boron nitride. The other is that nitrogen atoms desorbs at a lower rate, since the simultaneous Auger emission of two electrons required to neutralize a nitrogen ion, is less probable than the ordinary Auger process neutralizing an oxygen ion. To explain the observed EED of nitrogen atoms from the BN surface, desorption inherent to preferably covalence-bond systems cannot be totally excluded.

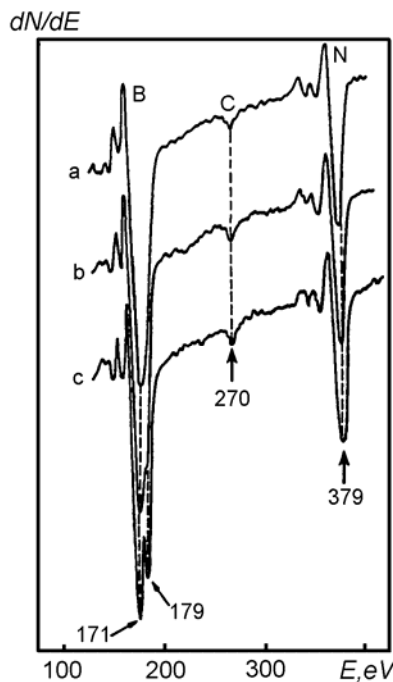


Figure 4. Auger spectra measured for the boron nitride surface at $T = 1200 \text{ K}$ after electron irradiation with the doses $D = 0$ (a), $8 \cdot 10^{19}$ (b), and $5 \cdot 10^{20} \text{ cm}^{-2}$ (c).

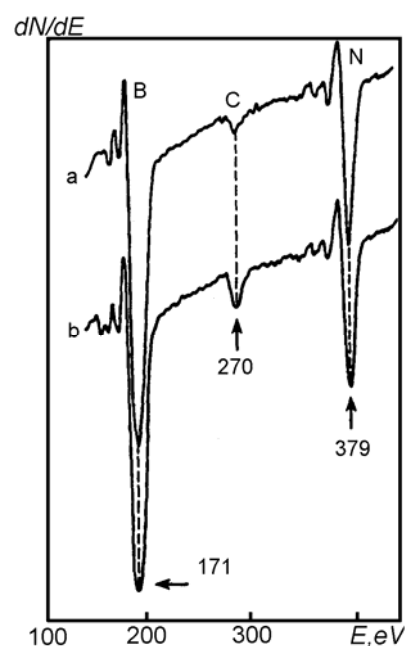


Figure 5. The same as in fig. 4 at $T = 300 \text{ K}$ before (a) and after (b) electron irradiation with the dose of $5 \cdot 10^{20} \text{ cm}^{-2}$.

B. Investigation of BN+Si₃N₄ Ceramic

In fig.6 one can see a differentiated Auger spectrum of BN+Si₃N₄ ceramic under $T=300$ K measured before electron radiation (doze of radiation $D=0$).

From fig.6 one can see that energetic position of the main Auger lines (B – 179 eV, C – 270 eV, N – 379 eV, O – 510 eV) corresponds to the etalon spectrums. At the same time the disposition of Si main line in LMM-series (81 eV) testifies that there are chemical bounds between Si and N.

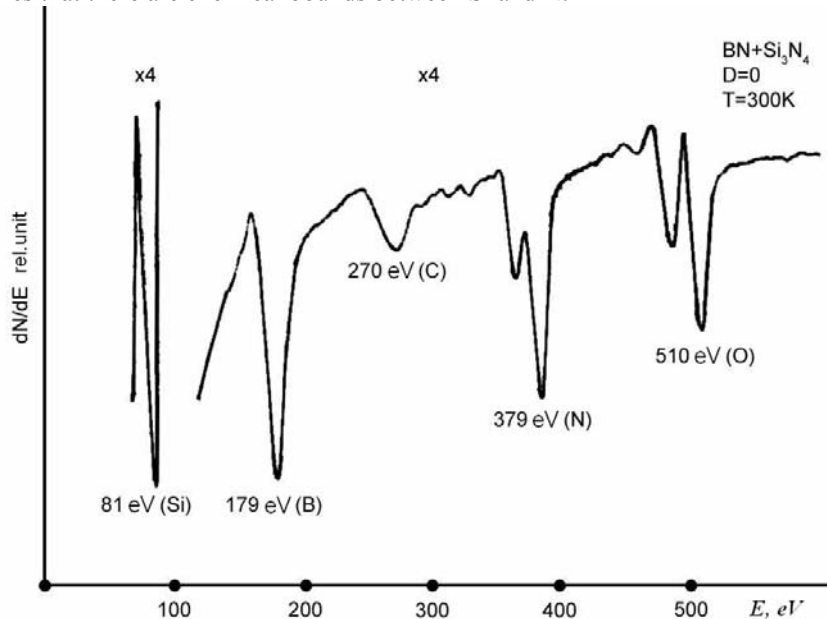


Figure 6. Energetic spectrum of Auger electrons from BN+Si₃N₄ ceramic under $T=300$ K measured before electron irradiation.

After sample irradiation by the electrons with energy 1-3 keV and dozes $D = 5 \cdot 10^{19} \text{cm}^{-2} - 2 \cdot 10^{20} \text{cm}^{-2}$ the spectrums of the main Auger lines were differ a few from the initial one (fig.6), but energetic position of the main Auger lines were practically the same with doze increase (fig.7 and 8).

It is differ from data represented in fig.7 by the following: after heating and simultaneous radiation, LMM line displaces towards greater energies (up to 91 eV) that is typical for pure Si. As an example, in fig. 9 it is shown Auger spectrum obtained after radiation with great doze $D=2 \cdot 10^{20} \text{cm}^{-2}$.

In fig. 10 one can see the spectrum from sample area, which was under the same temperature conditions, but was not subjected to electron action.

From the energetic point of view fig.9 has the same view that it is for the case of long-time radiation. It is necessary to point out that the line Si (91 eV) corresponds to the same position on the energy scale. The spectrum is differ only by Auger – picks amplitudes that is occurred due to the fact that carbon-containing compounds content increases on the surface under long-time electron bombardment. Great increase of carbon KLL line (270 eV) is testified it.

Viewing changes in the spectrums probably due to nitrogen desorption from sample surface, so the layer enriched by “pure” silicon is formed. As far as non-irradiated areas behave themselves by the same way, it is possible to assume that the process is caused by thermal action.

In contrast to silicon we did not see any changes in boron line (179 eV) form and position. It should be expected as far as hexagonal BN has high radiation-ability against electrons, and besides, it is thermo-stable.

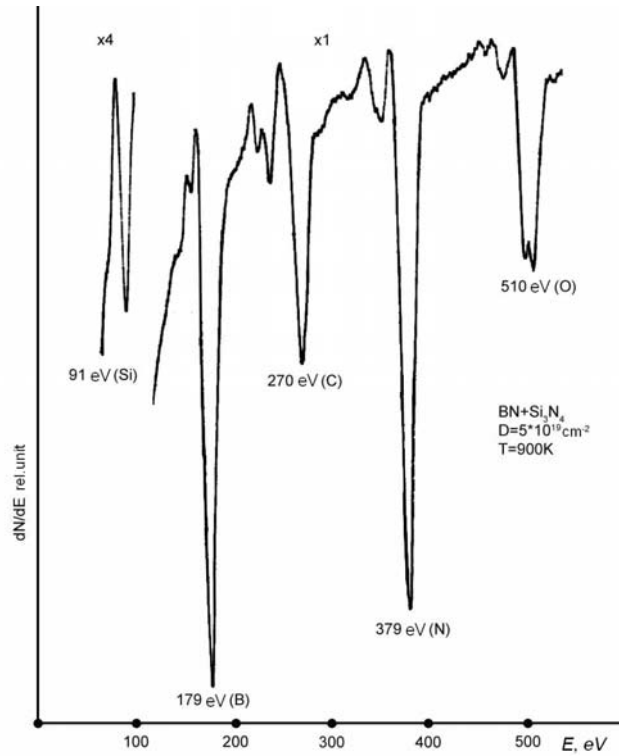


Figure 7. Energetic spectrum of Auger electrons from $\text{BN}+\text{Si}_3\text{N}_4$ ceramic under $T=900\text{K}$ after electron irradiation with energy $E=3\text{ keV}$, dose $D=5\cdot 10^{19}\text{ cm}^{-2}$.

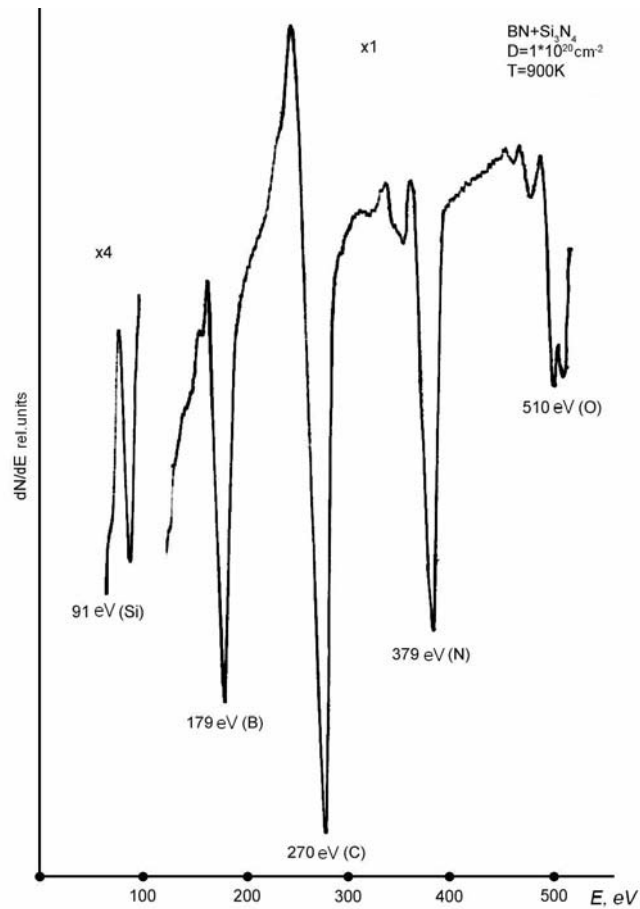


Figure 8. Energetic spectrum of Auger electrons from $\text{BN}+\text{Si}_3\text{N}_4$ ceramic under $T=900\text{K}$ after electron irradiation with energy $E=3\text{ keV}$, dose $D=1\cdot 10^{20}\text{ cm}^{-2}$.

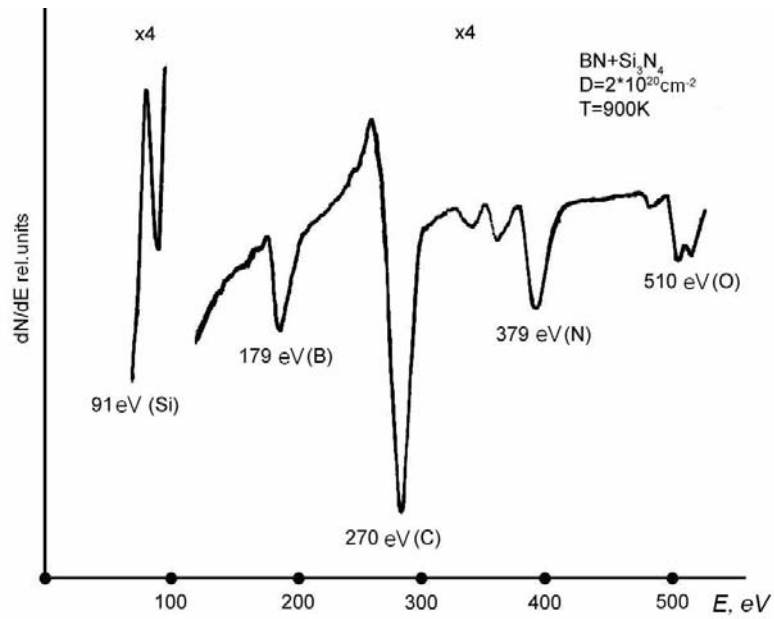


Figure 9. Energetic spectrum of Auger electrons from $\text{BN}+\text{Si}_3\text{N}_4$ ceramic under $T=900\text{K}$ after electron irradiation with energy $E=3\text{ keV}$, dose $D=2\cdot 10^{20}\text{ cm}^{-2}$.

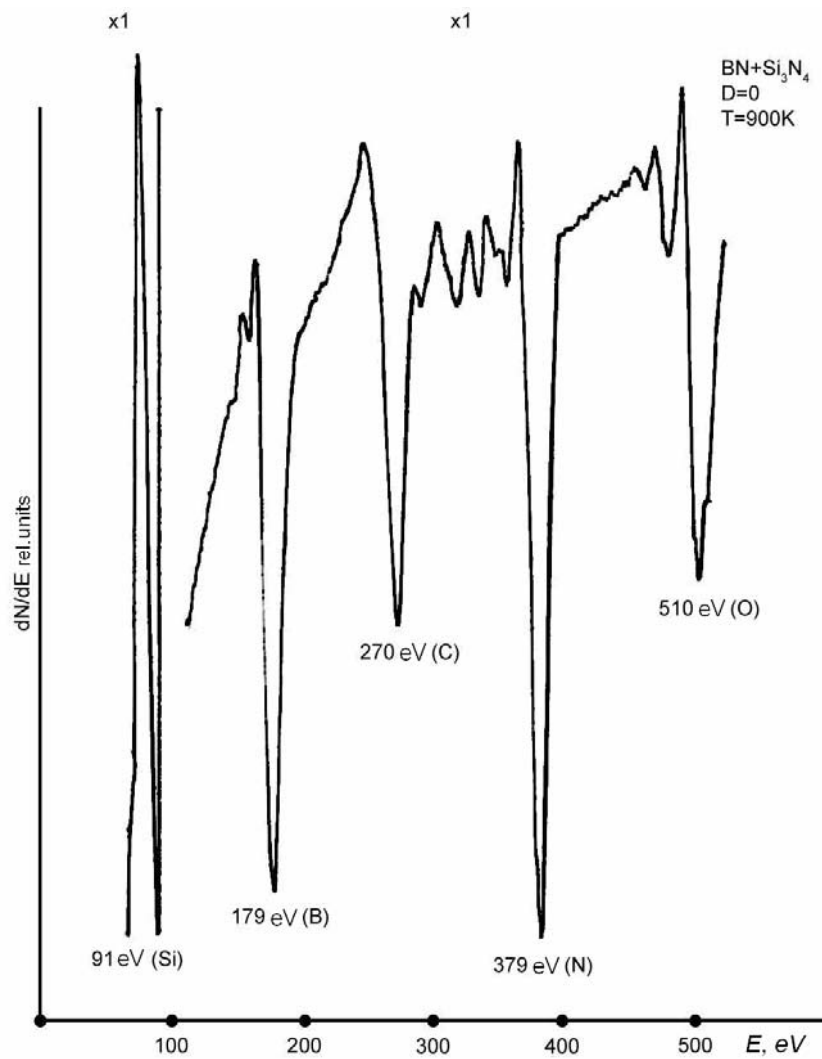


Figure 10. Energetic spectrum of Auger electrons from $\text{BN}+\text{Si}_3\text{N}_4$ ceramic under $T=900\text{K}$ without electron irradiation.

C. Investigation of BN+SiO₂ Ceramic

For BN+SiO₂ ceramic it was obtained the results a few differ from the results obtained for BN+Si₃N₄ ceramic.

In fig. 11 it is shown an Auger spectrum obtained under the same conditions that the spectrum represented in fig.6 (fresh chip of ceramic).

There is no any displacement of Auger B, N, C and Si (fig.12 and 13) lines with electron radiation dose ($5 \cdot 10^{19} \text{ cm}^{-2} - 2 \cdot 10^{20} \text{ cm}^{-2}$) increasing as it was taken place at the previous case.

At the same time the main line of Si LMM series displaced with dose increasing from 81 eV under $D=5 \cdot 10^{19} \text{ cm}^{-2}$ up to 87 eV under $D=2 \cdot 10^{20} \text{ cm}^{-2}$. In fig.14 it is represented the spectrum only under maximum dose of radiation.

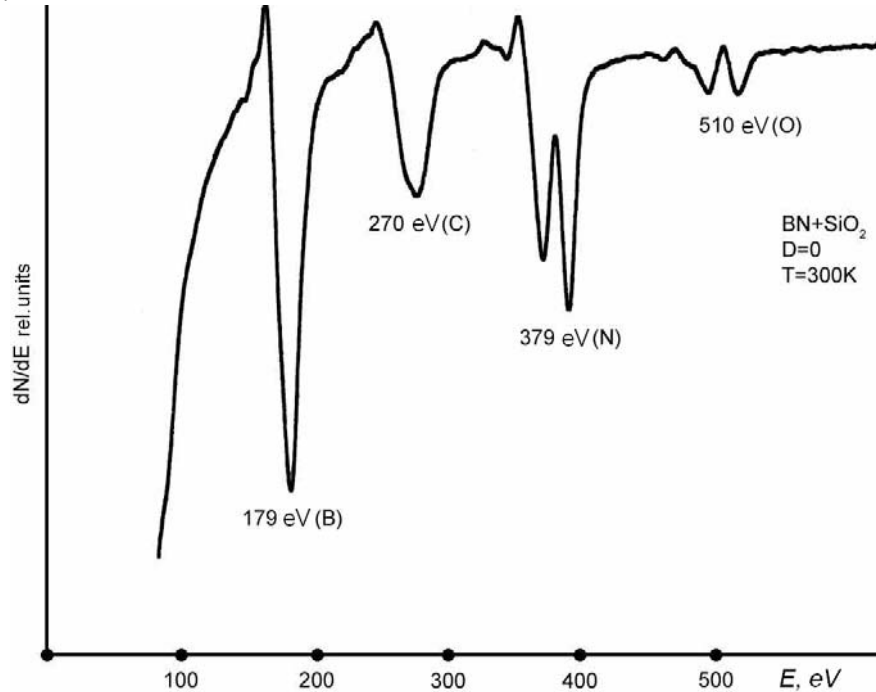


Figure 11. Energetic spectrum for Auger – electrons coming out of BN+SiO₂ ceramic under $T=300\text{K}$ measured before electron irradiation.

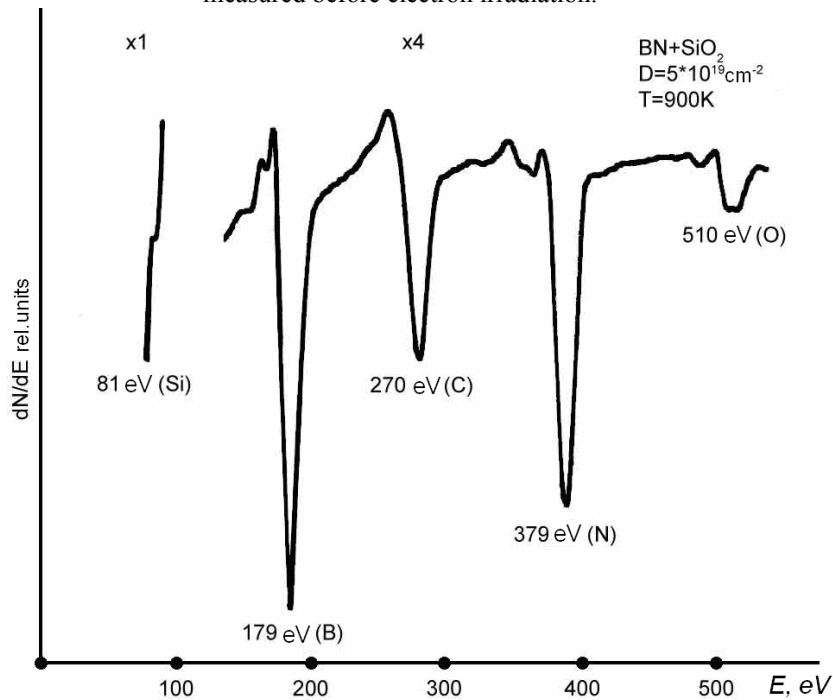


Figure 12. Energetic spectrum for Auger – electrons coming out of BN+SiO₂ ceramic under $T=900\text{K}$ measured after electron irradiation with energy $E = 3 \text{ keV}$, dose $D = 5 \cdot 10^{19} \text{ cm}^{-2}$.

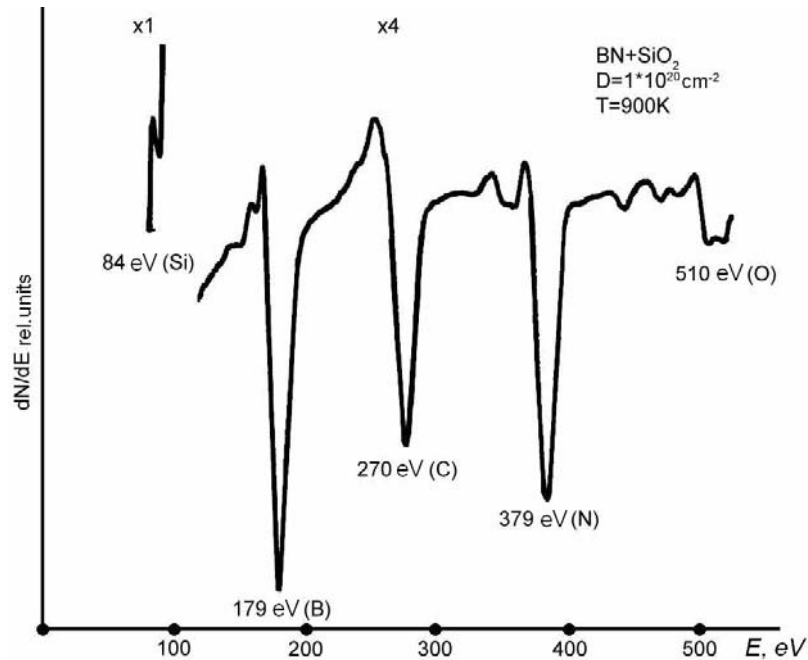


Figure 13. Energetic spectrum for Auger – electrons coming out of BN+SiO₂ ceramic under $T=900\text{K}$ measured after electron irradiation with energy $E=3\text{ keV}$, dose $D=1\cdot 10^{20}\text{ cm}^{-2}$.

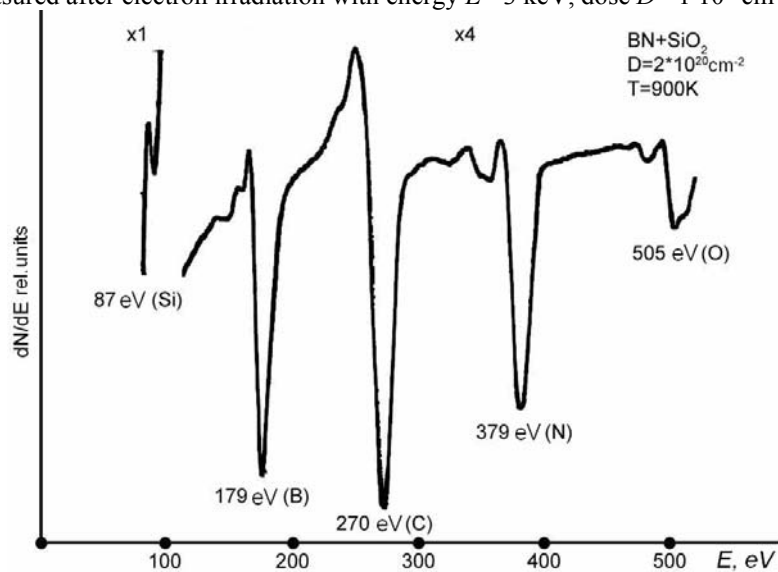


Figure 14. Energetic spectrum for Auger – electrons coming out of BN+SiO₂ ceramic under $T=900\text{K}$ measured after electron irradiation with energy $E=3\text{ keV}$, dose $D=2\cdot 10^{20}\text{ cm}^{-2}$.

Totally differ result was obtained for the non-radiated area of the sample, which was under the same temperatures that it was for the radiated surface (fig.15).

The main Si line of LMM series (79 eV) was in position close to the same line after radiation with dose $D=5\cdot 10^{19}\text{ cm}^{-2}$ (81 eV). Unfortunately we were unable to compare this spectrum area with data for the fresh chip, for which this line was not observed at all that is due to surfaced contamination and small concentration of SiO₂ (~ 10 %) in BN+SiO₂ ceramic.

The obtained results show that the object is resistant against temperature and that the surface destructs are insufficient due to electron-stimulated desorption of oxygen. The obtained estimations show that EED cross section is not more than 10^{-20} cm^2 .

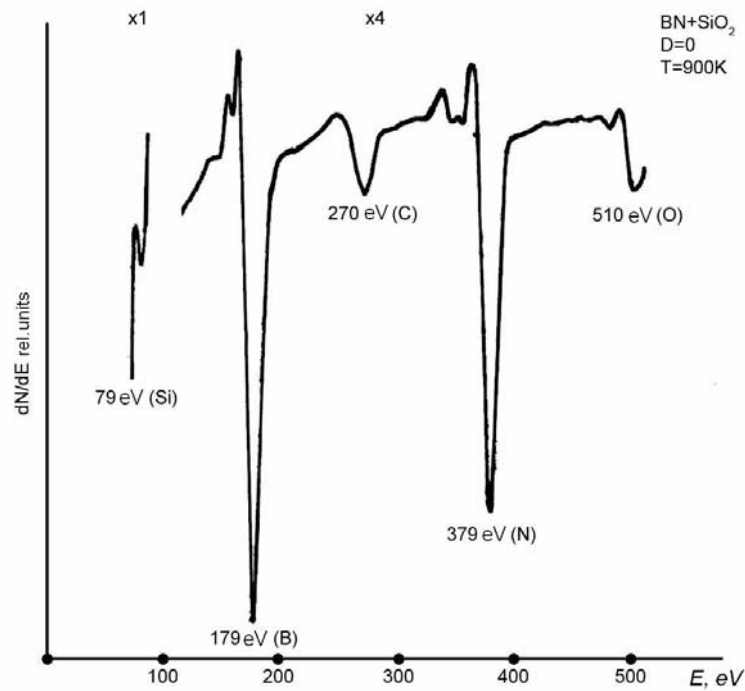


Figure 15. Energetic spectrum for Auger – electrons coming out of BN+SiO₂ ceramic under $T=900\text{K}$ without electron irradiation.

IV. Conclusion

It was shown that only the samples of wurtzite BN were destructed under low-energy electron radiation under dose higher than 10^{20} cm^{-2} . Besides, during EED investigation of the samples consisting of the mixture: cubical (50%) and wurtzite (50%) modifications of BN, it was shown that low-energy electron action stimulates the desorption process of nitrogen atoms from the surface. The estimations concerning process cross section σ showed that under $T=1200 \text{ K}$ $\sigma=1.5 \cdot 10^{-22} \text{ cm}^2$, that is less approximately in one order than it is for typical EED cross sections for the surface of most oxides. Under less temperature we did not see a new Auger line. At the same time the carbon content increased greatly on the surface during electron radiation. Under high temperatures ($> 1600 \text{ K}$) there was a thermo – destruction of BN with nitrogen emission and surface metallization.

For BN+Si₃N₄ the viewing changes in the spectrums occur due to nitrogen desorption from sample surface, so the layer concentrated by “pure” silicon is formed. As far as non-irradiated areas behave themselves by the same way, it is possible to assume that the process is caused by thermal action.

For BN+SiO₂ the obtained results show that the object is resistant against temperature and that the surface destructs is insufficient due to electron-stimulated desorption of oxygen. The obtained estimations show that EED cross section is not more than 10^{-20} cm^2 .

Summarizing the experimental campaign authors can make the conclusion that under the typical values of electron energies in the SPT channel the electron-enhanced desorption have not play a vital part in the ceramic sputtering and therefore can be leave out during experimental and numerical simulation of SPT ceramic erosion.

Acknowledgments

This work was supported by INTAS under the Project #03 53 5607.

References

Periodicals

²Desorption Induced by Electronic Transitions-DIET 1. Springer Series in Chemical Physics, Vol.24. Berlin: Springer, 1983.

³Elovikov S.S., Sushkova Yu.V., et al. Poverhnnost. Fiz. Khim. Mekh. 1992, No.6, 99 (Phys. Chem. Mech. Surface).

⁴Sushkova Yu.V., Elovikov S.S., et al. Ibid., No. 12, 99.

⁵Elovikov S.S. et al. Ibid, 1994, No. 7, 13.

⁶Tazhieva G.R., Elovikov S.S., et al. Ibid. 1995, No. 11, 46.

⁷Rakhovskaya O.V., Elovikov S.S., et al. Surf. Sci. 1992, 274, 190.

- ⁸Knotek M.L., Feibelman P.J. *Ibid.* 1979, 90, 78.
- ⁹Ramaker D.E. In: *Desorption Induced by Electronic Transitions—DIET 1*. Springer Series in Chemical Physics. Vol.24. Berlin: Springer, 1983, p. 70.
- ¹⁰Feibelman P.J. *Surf. Sci.* 1981, 102(2/3), L01.
- ¹¹Elovikov S.S., Eltekov V.A., et al. *J. Nucl. Mater.* 1994, 212-215, 1335.
- ¹²Eltekov V.A., Elovikov S.S., et al. *Radiat. Eff.* 1995, 133, 107.
- ¹³Pilyankevich O.M. *Dokl. Akad. Nauk UkrSSR* 1975, 2, 170 (Rep. Ukr. Acad. Sci.).
- ¹⁵Fomichev V.A. *Fit. Tverd. Tela* 1971,13(3), 907 (Sov. Phys.-Solid State).
- ¹⁶Fomichev V.A. *Bull. Acad. Sci. USSR, Phys. Ser.* 1967, 31 (6).
- ¹⁷Hamrin K., Johanson G., et al. *Phys. Scripta* 1970, 1, 277.
- ¹⁸Hanke G. and Muller K. *Surf. Sci.* 1985, 152/153,902.

Books

- ¹Morozov A.I. *Introduction into Plasma Dynamic*. Moscow: PhIZMATLIT, 2006 [in Russian].
- ¹⁴Harrison U.A. In: *Electronic Structure and Properties of Solids: Physics of Chemical Bond*. Vol.1. Moscow: Mir, 1983, p. 37 [in Russian].